

A novel multiple flow direction algorithm for computing the topographic wetness index

Bin Yong, Li-Liang Ren, Yang Hong, Jonathan J. Gourley, Xi Chen, You-Jing Zhang, Xiao-Li Yang, Zeng-Xin Zhang and Wei-Guang Wang

ABSTRACT

The topographic wetness index (TWI), frequently used in approximately characterizing the spatial distribution of soil moisture and surface saturation within a watershed, has been widely applied in topography-related geographical processes and hydrological models. However, it is still questionable whether the current algorithms of TWI can adequately model the spatial distribution of topographic characteristics. Based upon the widely-used multiple flow direction approach (MFD), a novel MFD algorithm (NMFD) is proposed for improving the TWI derivation using a Digital Elevation Model (DEM) in this study. Compared with MFD, NMFD improves the mathematical equations of the contributing area and more precisely calculates the effective contour length. Additionally, a varying exponent strategy is adopted to dynamically determine the downslope flow-partition exponent. Finally, a flow-direction tracking method is employed to address grid cells in flat terrain. The NMFD algorithm is first applied to a catchment located upstream of the Hanjiang River in China to demonstrate its accuracy and improvements. Then NMFD is quantitatively evaluated by using four types of artificial mathematical surfaces. The results indicate that the error generated by NMFD is generally lower than that computed by MFD, and NMFD is able to more accurately represent the hydrological similarity of watersheds.

Key words | flow partition, hydrological model, multiple flow direction algorithm, topographic wetness index

Bin Yong
Li-Liang Ren (corresponding author)
Xi Chen
Xiao-Li Yang
Zeng-Xin Zhang
Wei-Guang Wang
 State Key Laboratory of Hydrology-Water Resources and Hydraulic Engineering, Hohai University, Nanjing 210098, China
 E-mail: rll@hhu.edu.cn; njrll9999@126.com

Bin Yong
You-Jing Zhang
 School of Earth Sciences and Engineering, Hohai University, Nanjing 210098, China

Bin Yong
 State Key Laboratory of Water Resources and Hydropower Engineering Science, Wuhan University, Wuhan 430072, China

Yang Hong
 School of Civil Engineering and Environmental Sciences, University of Oklahoma, Norman, OK 73019, USA

Jonathan J. Gourley
 NOAA/National Severe Storm Laboratory, Norman, OK 73072, USA

INTRODUCTION

The topographic wetness index (TWI), originally defined in TOPMODEL (Beven & Kirkby 1979) to estimate the spatial distribution of variable source areas (Quinn *et al.* 1995) and predict local variations in water table depths (Brasington & Richards 1998) within a watershed, has been widely used to study the effects of topography on hydrologic processes at basin scale (Beven *et al.* 1984; Ambroise *et al.* 1996; Beven 1997; Chang & Lee 2008; Pradhan *et al.* 2008; Chen *et al.* 2010). Due to its simple but physically based nature as well as its potential to couple with groundwater variability in time and space, the TWI

concept has been implemented in several hydroecological-atmosphere models and topography-based land-surface process schemes used in regional climate models (RCMs) or global climate models (GCMs) (Famiglietti & Wood 1994; Stieglitz *et al.* 1997; Koster *et al.* 2000; Chen & Kumar 2001; Niu & Yang 2003; Yong *et al.* 2010). Today, TWI is regarded as a key index for modelling topography-based hydrological processes from catchment scale to regional or global scale (Niu *et al.* 2005; Bohn *et al.* 2007; Zushi 2007; Clark & Gedney 2008; Harris & Hossain 2008; Yong *et al.* 2009).

The computation of TWI in TOPMODEL is made from a gridded DEM according to the formula:

$$\text{TWI} = \ln(\alpha/\tan \beta)$$

where α is the upslope contributing area per unit contour length (or Specific Catchment Area, SCA) and β is the local slope angle at the point.

Current geographic information system (GIS-) based calculation methods for TWI can be classified into two main types according to the choice of flow direction schemes: single flow direction (SFD) and multiple flow direction (MFD) algorithms (Wolock & McCabe 1995). In the SFD algorithm, it is assumed that the subsurface flow at every grid cell occurs only in the steepest downslope direction. Given this simplification, the SFD algorithm has been widely used in DEM data analysis and GIS software, such as the D8 algorithm implemented in ARC/INFO. On the contrary, the MFD essentially assumes that the flow from a grid cell could drain into more than one downslope neighbouring pixel (Quinn et al. 1991). Many studies have shown that MFD is better than SFD, especially when the spatial pattern of upstream contributing area needs to be computed (Wolock & McCabe 1995; Pan et al. 2004). However, the existing MFD algorithm also has some disadvantages in computing the effective contributing drainage area and dealing with grid cells in flat terrain. Moreover, MFD generally employs a fixed-exponent strategy to determine the fractions draining to all downslope neighbours, which cannot effectively account for the impact of local terrain conditions on the dispersion of local flow.

In this paper, a GIS-based novel multiple flow direction (NMFD) algorithm is developed to address the above-mentioned problems of MFD in the TWI calculation. First, the basic theory of MFD and NMFD are described. The new algorithm is then applied to a catchment within China's Hanjiang River basin. Finally, NMFD is quantitatively evaluated using four types of mathematical surfaces and their theoretical 'true' values of SCA and TWI. Results of this study will be potentially beneficial not only for accurate application of TWI to watershed feature extraction and hydrological modelling, but also for understanding the formation mechanism of geomorphology and soil erosion.

CURRENT COMMONLY USED MFD

When the MFD algorithm is applied, every grid cell should have at least one downslope neighbouring pixel. The fraction of the area draining through the current cell to each downslope direction is proportional to the slope gradient of each downhill flow path, so that steeper gradients will attract more water from the upstream contributing area (Quinn et al. 1991).

Under the MFD algorithm, the calculation of α in $\ln(\alpha/\tan \beta)$ can be described by the following four equations. According to Quinn et al. (1991), α is defined as:

$$\alpha = A / \sum_{j=1}^n L_j \quad (1)$$

where A is the total area draining into each cell and L_j is the effective contour length of the cell boundary between the current cell and its j th downslope neighbouring cell. The value of L_j is set to one-half the grid cell size for cells in cardinal directions (illustrated as L_1 and L_5 in Figure 1), and 0.354 times the grid cell size for cells in diagonal directions (such as L_2 and L_4 in Figure 1).

The local slope angle in the downslope direction, $\tan \beta$, is computed as:

$$\tan \beta = \frac{\sum_{j=1}^n (\tan \beta_j L_j)}{\sum_{j=1}^n L_j} \quad (2)$$

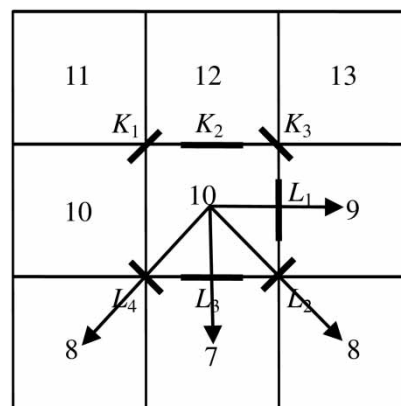


Figure 1 | An example of a simulated flow partition on DEM using the multiple flow direction algorithm. Numbers in cells are elevation values.

where $\tan \beta_j$ is the slope gradient between the current cell and its j th downslope neighbouring cell. Combining Equations (1) and (2), $\ln(\alpha/\tan \beta)$ can be defined as:

$$\ln(\alpha/\tan \beta) = \ln \left(A / \sum_{j=1}^n (\tan \beta_j L_j) \right) \quad (3)$$

The total upslope area of the current cell is distributed to its downslope neighbouring cells as:

$$\Delta A_i = \frac{A(\tan \beta_i L_i)}{\sum_{j=1}^n (\tan \beta_j L_j)} \quad (4)$$

where ΔA_i is the drainage area passed from the current cell onto its downslope neighbouring cell i .

THE NOVEL MULTIPLE FLOW DIRECTION ALGORITHM (NMFD)

Improved representation of cumulative upstream contributing area

In the original MFD algorithm, the physical description of α is the total upslope area (A) per unit contour length draining from upstream cells to the current cell, which in fact reflects the tendency of upslope water to accumulate at the current cell in the catchment. It is therefore not reasonable that the effective contour lengths between the current cell and its downslope neighbouring cells (e.g. L_1 , L_2 , L_3 and L_4 in Figure 1) were used to determine α in Quinn *et al.* (1991). The effective contour lengths of the grid cell boundaries for calculating the upslope contributing area (α) should be between upslope cells and current cell (e.g. K_1 , K_2 and K_3 in Figure 1) rather than between the current cell and downslope cells. Thus, in NMFD, Equation (1) is modified to become:

$$\alpha = \frac{A}{\sum_{i=1}^m K_i} \quad (5)$$

where K_i is the effective contour length of the grid cell boundary between the current cell and its i th upslope neighbouring cell.

The term $\tan \beta$ is the local slope angle of the current cell, which reflects the tendency of gravitational forces to move

upslope water from the current cell to downslope neighbouring cells. Equation (2) for calculating $\tan \beta$ is therefore still relevant under NMFD. Substituting Equation (5) into Equation (1), Equation (3) then becomes:

$$\ln(\alpha/\tan \beta) = \ln \left(A / \sum_{j=1}^n (\tan \beta_j L_j) \right) + \ln \left(\sum_{j=1}^n L_j / \sum_{i=1}^m K_i \right) \quad (6)$$

Used in NMFD, Equation (6) suggests that for any grid cell the difference between MFD- and NMFD-derived TWI is the additional term:

$$\ln \left(\sum_{j=1}^n L_j / \sum_{i=1}^m K_i \right)$$

The maximum difference will occur when upslope water enters into the current cell from only one upslope neighbouring cell at the diagonal direction and then diverges into seven neighbouring downslope cells. The largest negative difference occurs inversely, i.e. where water converges on the current cell from seven upslope cells and then continues to a single downslope cell at the diagonal direction. If L_j is set to $0.5 \times \Delta x$ for cardinal boundaries and to $0.354 \times \Delta x$ for diagonal boundaries as it was originally assumed by Quinn *et al.* (1991), the values of the above expression are 2.158 and -2.158 for the above two extreme cases, respectively.

Additionally, in MFD the calculated total drainage area contributing to the downslope cells does not include the area of the current cell. This shortcoming will result in errors in the iterative programming for the computation of TWI. It is therefore necessary to modify Equation (4) as:

$$\Delta A_i = (A + \Delta x^2) \frac{\tan \beta_i L_i}{\sum_{j=1}^n (\tan \beta_j L_j)} \quad (7)$$

where Δx is the grid cell size of the DEM.

Accurate calculation of effective contour length

In the MFD algorithm, each flow direction is weighted by the downward elevation gradient multiplied by the effective

contour length L_j . Figure 1 shows that the downslope directions are split into cardinal and diagonal flow directions, so the values of L_j should be different in those two different flow directions. In Quinn et al. (1991), L_j was set to $0.5 \times \Delta x$ for boundaries with cardinal neighbouring downslope cells and to $0.354 \times \Delta x$ for boundaries with diagonal neighbouring downslope cells. Quinn et al. (1991) indicated that the contour length values were estimated subjectively. Later, Wolock & McCabe (1995) simply defined 0.6 and 0.4 as the weighting factor of the contour length for cardinal and diagonal directions, respectively. Their reasoning was based on the fact that the sum of the current cell's effective contour lengths should equal the total boundary length between the current cell and all of its neighbouring downslope cells (Wolock & McCabe 1995). This assumption did not yield accurate results from experimental analysis or theoretical derivation.

Based on the impermeable conical surface concept in Giuseppe & Aurelia (1997), a simple and adaptive geometric methodology – i.e. conical surface inscribed circle (CSIC) approach – is proposed to accurately calculate the effective contour length in different downslope directions. To illustrate this computational method clearly, the lower-right four cells of Figure 1 are extracted (see Figure 2) and two tangent lines starting from the central point of the current cell can be drawn for the inscribed circle of the cardinal downslope cell A_3 (or A_1). According to the assumption of Giuseppe & Aurelia (1997) that the flows always follow the impermeable conical surface to drain evenly into downslope cells, in

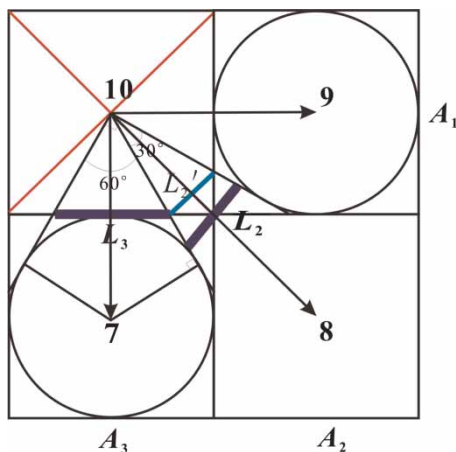


Figure 2 | Conical surface inscribed circle approach for accurately calculating the effective contour length.

our study it can be seen that the flows between two tangent lines of the cardinal-inscribed circle will drain through the line segment L_3 into the cardinal cell A_3 and flows passing through L_2 will drain into the diagonal downslope direction cell A_2 . In fact, L_3 and L_2 are the effective contour lengths we have been seeking. For the DEMs with regular square meshes, the accurate values of the effective contour length can be readily computed. In NMFD, the weighting factor of the effective contour length is 0.577 and 0.379 for the cardinal and diagonal flow directions, respectively.

Implementation of varying flow-partition exponent strategy

Although some computing deficiencies of the effective cumulative area have been remedied through the above modifications, another important problem still remains unresolved; i.e., the fixed-exponent strategy to model the flow partitioning used in MFD. In practice, the fixed-exponent strategy is unsuitable when the complex terrain of some watersheds includes both convergence and divergence because the exponent cannot be altered in response to local terrain conditions. In this study, a straightforward adaptive scheme proposed by Qin et al. (2007) is adopted to dynamically determine the downslope flow-partition exponent and accurately compute the TWI distribution under various terrain characteristics. According to the approach of Qin et al. (2007), Equation (7) can be modified to the following expression for computing ΔA_i :

$$\Delta A_i = (A + \Delta x^2) \frac{(\tan \beta_i)^{f(e)} L_i}{\sum_{j=1}^n (\tan \beta_j)^{f(e)} L_j} \quad (8)$$

Under MFD, which sets the flow-partition exponent function $f(e) = 1$, the partition of the downslope flow cannot adapt to varying local terrain. Here, e is the tangent value of the maximum downslope slope angle and $f(e)$ is a linear function of e , rather than a fixed constant value. A detailed study on the determination of $f(e)$ has been reported in a previous paper (Qin et al. 2007). According to Qin et al. (2007), the final form of $f(e)$ is as follows:

$$f(e) = 8.9 \times \min(e, 1) + 1.1 \quad (9)$$

where $\min(e, 1)$ is the minimum of e and 1 and the domain of $f(e)$ is defined as [1.1,10].

Freeman (1991) tested and analysed the cases of $f(e) = 1, 1.1$ and 1.25 , respectively. The study concluded that $f(e) = 1.1$ is the optimum value for the complete divergence of flow, not the previously accepted value of 1. Moreover, both Holmgren (1994) and Quinn *et al.* (1995) considered that $f(e) = 10$ should be the best choice for modelling the SFD, which can be regarded as the complete convergence of flow. Equation (9) shows that the values of 1.1 and 10 are the upper and lower bounds of $f(e)$. A variable flow-partition exponent, which is now implemented in NMFD, should therefore be more rational and precise than the fixed-exponent strategy used in MFD previously.

Determination of slopes in flat areas using the tracking flow direction method

Because DEMs often contain flat areas where the TWI cannot be directly calculated, the utilization of slopes from nearby cells with the same elevation is often required for various TWI computation algorithms. Wolock & McCabe (1995) suggested that the slope gradient of cells in flat areas be set to $(0.5 \times \text{vertical resolution}) / (\text{horizontal resolution})$. This method is straightforward, but not robust in low-relief areas.

In NMFD, the tracking flow direction (TFD) method recommended by Pan *et al.* (2004) is used to process cells in flat areas. The example in Figure 3 demonstrates the basic idea of this algorithm. TFD starts from cell A and follows the flow direction determined by a widely used approach of Jenson & Domingue (1988), which has been adopted as the 'FLOW-DIRECTION' function in ARC/INFO software. The nearest cell B with a lower elevation can then be found. The tangent value at cell A, $\tan \beta_A$, is computed as:

$$\tan \beta_A = \frac{(e_A - e_B)}{\sum_{i=1}^T D_i \Delta x} \quad (10)$$

(i.e. the ratio of the elevation difference to the length of the flow path between A and B) where:

$$D_i = \begin{cases} \sqrt{2}, & \text{when diagonal flow direction} \\ 1, & \text{when cardinal flow direction} \end{cases}$$

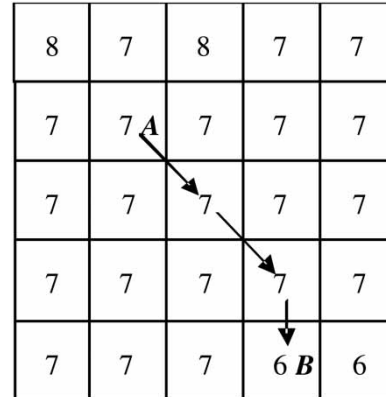


Figure 3 | An example of the TFD method for computing the slopes in flat areas.

and where e_A and e_B are the elevation of cell A and B, respectively. D_i is the length coefficient of two neighbouring cells at the i th iterative calculation when using the approach of Jenson & Domingue (1988) to derive the flow directions, and is equal to $\sqrt{2}$ and 1 for diagonal and cardinal flow directions, respectively. T is the total number of iterations from cell A to B. For example, the slope value between A and B in Figure 3 is equal to:

$$\frac{(7 - 6)}{(2\sqrt{2} + 1)\Delta x}$$

If the slope tangent of a certain cell is always zero, the minimum of all slope values will be assigned to this cell after the end of the iterative calculation program. As TFD can produce smaller slope values in flat areas, it is more accurate than the method of Wolock & McCabe (1995) under most terrain conditions.

COMPARISON OF MFD AND NMFD COMPUTED IN A STUDY CATCHMENT

A comparison between the different flow direction algorithms is necessary because they can produce very different results even for the same DEM (Wilson & Gallant 2000). To assess the differences between NMFD and MFD, the Baohe catchment located in the southwest Shanxi Province in China is selected as the experimental area (see Figure 4). This catchment with a drainage area of 2,413 km² above the Jiangkou hydrological station lies upstream of the Hanjiang

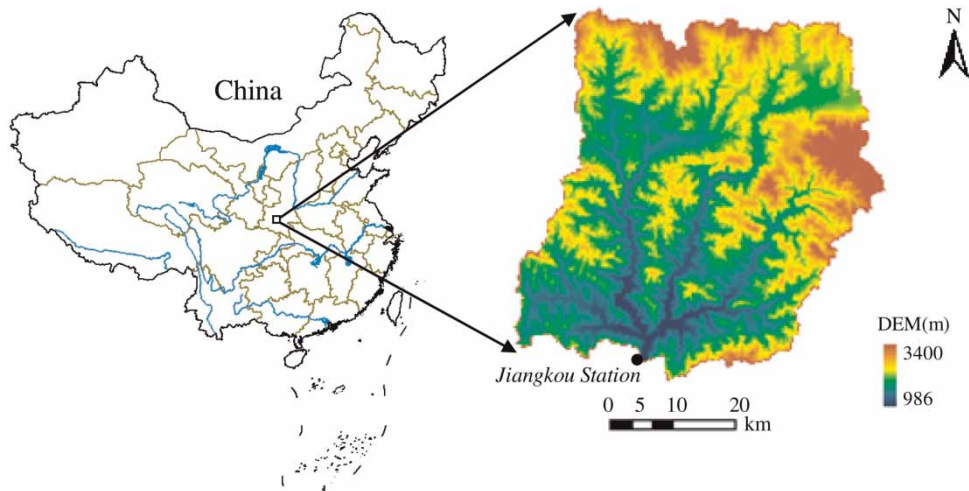


Figure 4 | Location of the Baohe catchment and its DEM (60 m × 60 m) used in this study.

River, which is one of the largest branches of the Yangtze River. It extends between 33°38'03" and 34°1'08" N and 106°48'15" and 107°25'34" E with a typical subtropical humid climate. A 60 × 60 m DEM with a UTM projection (Zone 48) and coordinate system of WGS84 is digitized from the thematic topography map at the 1:100,000 scale, which was provided by the local authority.

The Baohe catchment has a varying and complicated topography with elevations ranging from 986 m above sea level at the channel outlet to 3,400 m in the upstream mountainous area. The average annual temperature, precipitation

and potential evaporation are approximately 16 °C, 1,400 and 848 mm, respectively. The vegetative cover is about 70% forested and grassland, with the remainder being mainly cropland. The predominant soil types include yellow-brown earths, brown earths and cinnamon soils.

First, the two multiple flow direction algorithms MFD and NMFD were programmed in Fortran90 and applied to compute TWI values over the Baohe catchment (Figure 5(a) and (b)), respectively. Although the spatial distribution of TWI generated by NMFD looks similar to that of MFD, the NMFD algorithm produced a distribution with a smoother

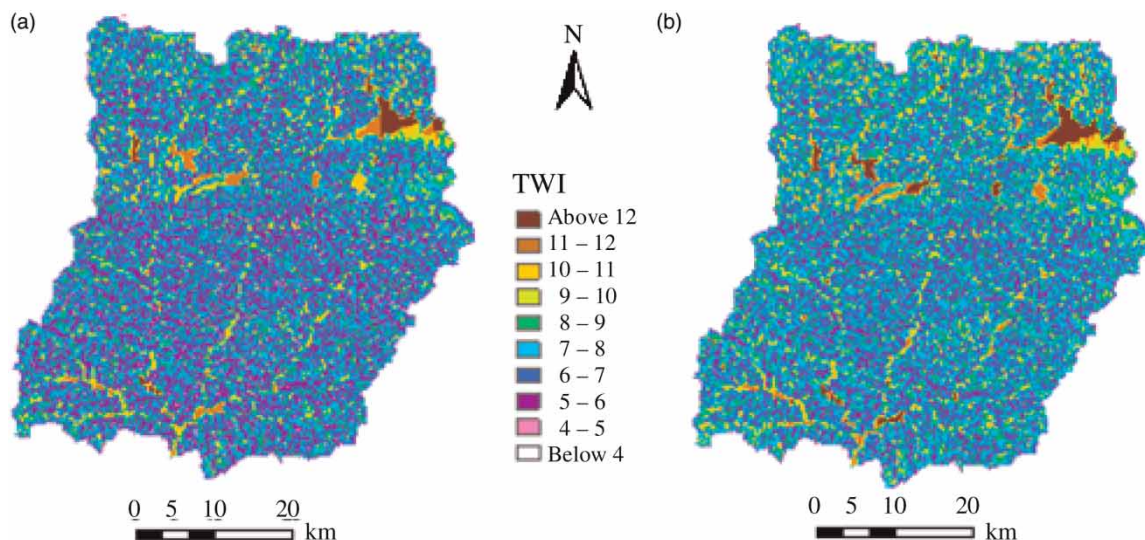


Figure 5 | Spatial distributions of TWI computed by (a) the MFD algorithm and (b) the NMFD algorithm in the Baohe catchment.

pattern and slightly higher TWI values. The TWIs computed by NMFD have higher values than those by the MFD especially in the foothills and narrower, headwater channels. This phenomenon is due to local terrain with smaller slopes, or due to wide and flat valleys where the soil moisture values are normally larger (i.e. higher TWI). Overall, NMFD can more realistically retrieve the TWI spatial distribution and better indicate the status ('dry' or 'wet') of the soil moisture conditions in the study area compared with MFD results.

The spatial distribution of the TWI values can be described by their maximum, minimum, mean, variance and skew values (Table 1). Compared with MFD, the changes in the method used to compute TWI in NMFD mainly include improving the equations for deriving the upslope contributing area α (Equations (6) and (7)), fixing the values of the effective contour length (i.e. $0.577 \times \Delta x$ for the cardinal direction and $0.379 \times \Delta x$ for the diagonal direction), adopting the varying exponent strategy to model the flow partition (Equations (8) and (9)) and using the TFD method to determine the slope angle in flat areas (Equation (10)). Depending on the terrain, the above four changes might increase or decrease the TWI value for a given cell. For example, when Equation (6) is used to calculate TWI, the term:

$$\ln \left(\frac{\sum_{j=1}^n L_j}{\sum_{i=1}^m K_i} \right)$$

can vary from 2.207 to -2.207 for NMFD according to the different inflow and outflow paths. The symmetry of this term about zero likely results in self cancellation from different local terrain, and explains why there are only small differences between statistical comparisons from the two algorithms. However, the NMFD algorithm results in a TWI distribution with a slightly higher mean value and lower variance and skew values for the Baohe catchment

Table 1 | Statistical results of the $\ln(\alpha/\tan \beta)$ distribution computed using MFD and NMFD

| Algorithm | Min | Max | Mean | Variance | Skew |
|------------|------|-------|---------|----------|------|
| MFD | 3.06 | 15.54 | 7.15 | 2.90 | 1.70 |
| NMFD | 2.98 | 14.45 | 7.67 | 2.45 | 1.55 |
| Difference | 0.08 | 1.09 | -0.52 | 0.45 | 0.15 |

compared with MFD. This finding is consistent with the conclusion of Wolock (1995) that the mean TWI values computed by MFD are larger than SFD, while the variance and skew values are lower.

QUANTITATIVE EVALUATION OF NMFD USING ARTIFICIAL MATHEMATICAL SURFACES

To further assess the accuracy and effectiveness of NMFD, a more objective approach is necessary for quantitatively comparing the errors generated by MFD and NMFD. The most common method of evaluating the error is to apply various algorithms to the DEM of a catchment and then compare TWI with the ground measurements of soil moisture or saturation. However, such an evaluation method has serious deficiencies. Firstly, this method cannot give the 'true' value of the topographic parameters (e.g. α or $\ln(\alpha/\tan \beta)$) and only regards spatial patterns of values possessing physical realism as the standard reference, so that it is subject to human judgment (Zhou & Liu 2002).

Secondly, conclusions and results derived from a selected study area may not be transferable to other basins. Furthermore, derived TWI values depend on the accuracy of the DEM which is imperfect due to sampling errors, interpolation errors and/or representation errors. The errors produced by the algorithms could therefore be dominated and overshadowed by the DEM errors (Zhou & Liu 2004).

Finally, soil moisture or saturation is one of the most difficult state parameters to measure because of its large spatiotemporal variations with different soils, vegetation cover and atmospheric conditions that can change on hourly timescales. Observations of soil moisture or saturation might be approximately related to static TWI values, but they cannot be directly used to evaluate the accuracy of different flow direction algorithms.

In this section, standard artificial mathematical surfaces are used to quantitatively compare the performance of the MFD and NMFD algorithms. This method is attractive because using mathematical surface models with controlled parameters provides the theoretical 'true' value of a key topographic parameter (i.e. α in this paper) at any point, thus enabling an objective evaluation and comparison between different flow direction algorithms. Currently,

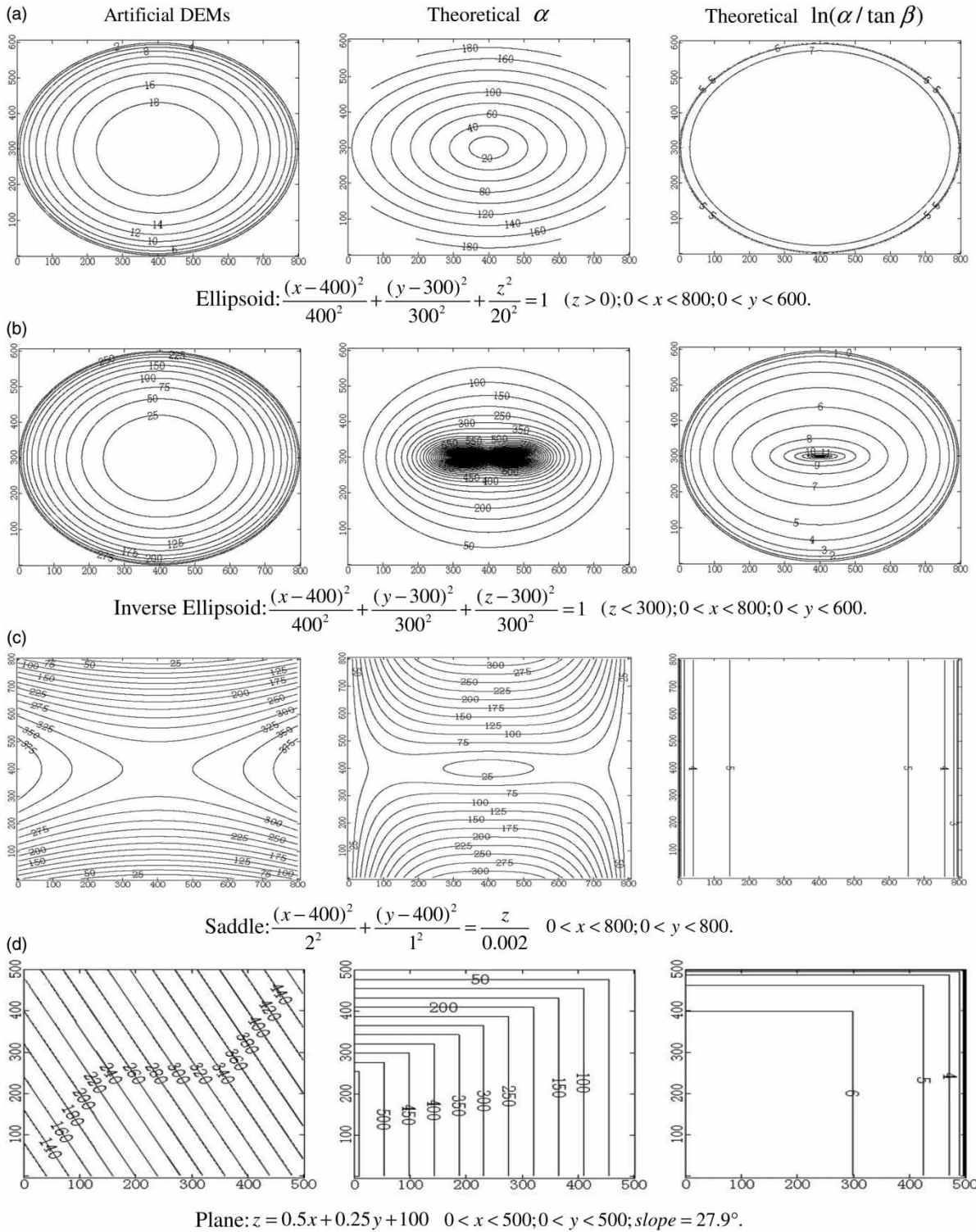


Figure 6 | Contour maps. Left column: artificial DEM surfaces; middle column: the theoretical α distributions; and right column: the theoretical $\ln(\alpha/\tan \beta)$ distributions of four typical mathematical surfaces: (a) ellipsoid; (b) inverse ellipsoid; (c) saddle; and (d) plane. These plots provide the standard ‘true’ values of α and $\ln(\alpha/\tan \beta)$, which are taken as the evaluating benchmarks for calculating the MFD and NMFD algorithm errors.

there are two quantitative methods with which artificial mathematical surfaces are used to estimate the error of the flow direction algorithms. One was proposed by Zhou & Liu (2002) and the other by Pan *et al.* (2004). The artificial surfaces created by Zhou & Liu (2002) included the saddle surface to represent the mountain ridge of a watershed. Additionally, the ellipsoid surface in Zhou & Liu (2002) was a better approximation to the convex slope terrain than the conical surface in Pan *et al.* (2004). Overall, the artificial DEM surface types proposed by Zhou & Liu (2002) were good approximations of the diverse topographies in a watershed. The method of Zhou & Liu (2002) is therefore used to create artificial mathematical surfaces in order to compare NMFD and MFD.

The core of the approach of Zhou & Liu (2002) was to construct four types of artificial surfaces (i.e. ellipsoid, inverse ellipsoid, saddle and plane) which can be represented by mathematical models. Comparing the theoretical values and the computed values of α and $\ln(\alpha/\tan \beta)$, the errors within each algorithm can be directly computed at each grid cell. This evaluation method can include various terrain conditions including divergent, convergent, ridge, planar, etc. Zhou & Liu (2002) gave a more detailed description of this approach.

Figure 6 depicts an example of the four mathematical models. Based on the artificial DEM surfaces and the theoretical α and $\ln(\alpha/\tan \beta)$ distributions (see Figure 6), the root mean square errors (RMSEs) of α and $\ln(\alpha/\tan \beta)$ are computed for MFD and NMFD, respectively. The RMSE of α ($RMSE_{\alpha}$) is computed as follows:

$$RMSE_{\alpha} = \sqrt{\frac{\sum_{i=1}^n (\alpha_{Ti} - \alpha_{Ci})^2}{n}} \quad (11)$$

where subscripts Ti and Ci represent the theoretical and computed α at the i th grid cell and n is the number of grid cells used for evaluation. The RMSE of the calculated topographic index ($RMSE_{TI}$) is:

$$RMSE_{TI} = \sqrt{\frac{\sum_{i=1}^n [\ln(\alpha/\tan \beta)_{Ti} - \ln(\alpha/\tan \beta)_{Ci}]^2}{n}} \quad (12)$$

Table 2 lists the $RMSE_{\alpha}$ and $RMSE_{TI}$ values computed for the four mathematical surfaces using MFD and NMFD.

Table 2 | RMSEs of α and $\ln(\alpha/\tan \beta)$ computed from four mathematical surfaces using the MFD and NMFD algorithms

| Surfaces | Algorithms | | | |
|-------------------|------------------------|---------|--------------------|-------|
| | $RMSE_{\alpha}$ MFD | NMFD | $RMSE_{TI}$ MFD | NMFD |
| Ellipsoid | 6.602 | 5.634 | 0.063 | 0.037 |
| Inverse ellipsoid | 500.513 | 398.732 | 0.081 | 0.109 |
| Saddle | 109.779 | 96.324 | 0.573 | 0.422 |
| Plane | 412.448 | 28.491 | 0.176 | 0.149 |

Both algorithms yield the smallest errors for the ellipsoid surface, which suggests that the multiple flow direction algorithm is more suitable for convex slopes. The most significant errors from both algorithms occur in estimating α for the inverse ellipsoid. This phenomenon might be partly due to the fact that this artificial surface has no drainage outlet.

Comparing the $RMSE_{\alpha}$ values from the two algorithms, NMFD yields lower errors than MFD under all evaluated artificial terrain conditions. Considering the RMSEs for $\ln(\alpha/\tan \beta)$, NMFD produces greater accuracy for three kinds of terrain conditions than MFD but not for the inverse ellipsoid surface. Note that the $RMSE_{\alpha}$ derived by MFD is approximately 15 times higher than NMFD. This is because MFD uses the fixed-exponent strategy ($f(e) = 1$) and does not accurately model convergent flows on terrain with straight slopes, while NMFD with the varying exponent strategy yields much lower error. In summary, the quantitative evaluation suggests that NMFD performs reasonably well and produces better results in a majority of the cases. Compared with MFD, NMFD can more accurately capture the spatial distribution of TWI and more reasonably reflect the hydrological similarity within a watershed.

CONCLUSIONS

TWI is a key index for modelling topography-dependent hydrological processes at small catchments and large basins, and provides for an estimate of the spatial distribution of soil moisture and surface saturation. Based on the MFD algorithm (Quinn *et al.* 1991), an improved scheme (i.e. NMFD) is proposed for more accurate computation of the TWI distribution in this study.

The key improvements include:

1. improving the equations of the classical MFD algorithm to more realistically compute the specific catchment area α ;
2. implementing a geometric methodology i.e. conical surface inscribed circle (CSIC) approach, to more accurately calculate the effective contour length in both cardinal and diagonal downslope directions;
3. adopting a varying exponent strategy for accurate modeling of flow partition; and
4. applying a flow-direction tracking method (i.e. TFD) to meticulously deal with grid cells in flat terrain.

The proposed NMFD algorithm was applied to the Baohe catchment in China to compute the spatial distribution of TWI. Four different types of mathematical surfaces were then used to quantitatively evaluate the calculated values of the specific catchment area and the topographic wetness index from the two different flow direction algorithms, based on the theoretical true values. Assessment of the results indicates that the spatial distribution of TWI computed by NMFD is more accurate and adaptable to various terrain conditions than the current, widely used MFD. To generalize the findings of this study and to realize its added value, exhaustive evaluations of the NMFD should be considered in future work by applying the NMFD algorithm to more complex terrain conditions, explicit TOPMODEL hydrologic modelling and even regional climate modelling studies.

ACKNOWLEDGEMENTS

This research was funded by the National Key Basic Research Program of China (2006CB400502) and the National Science Foundation for Young Scientists of China (40901017). This work was also financially supported by the 111 Project, Ministry of Education and State Administration of Foreign Experts Affairs of China (B08048), the Fundamental Research Funds for the Central Universities, the open study funds of State Key Laboratory of Water Resources and Hydropower Engineering Science (2008B039) and the Independent Innovation Project of State Key Laboratory of Hydrology-Water Resources and Hydraulic Engineering

(2009586512). The authors also acknowledge the partial support granted by the Key Project of Chinese Ministry of Education (308012) and the Program for Changjiang Scholars and Innovative Research Team in University, Chinese Ministry of Education (IRT0717). We extend our appreciation to the anonymous reviewers for their constructive suggestions on an earlier version of this paper.

REFERENCES

- Ambrose, B., Freer, J. & Beven, K. J. 1996 Towards a generalization of the TOPMODEL concepts: topographic indices of hydrological similarity. *Water Resour. Res.* **32**, 2135–2145.
- Beven, K. J. 1997 TOPMODEL: a critique. *Hydrol. Process.* **11**, 1069–1085.
- Beven, K. J. & Kirkby, M. J. 1979 A physically based, variable contributing area model of basin hydrology. *Hydrol. Sci. Bull.* **24** (1), 43–69.
- Beven, K. J., Kirkby, M. J., Schofield, N. & Tagg, A. 1984 Testing a physically-based flood forecasting model (TOPMODEL) for three U.K. catchments. *J. Hydrol.* **69**, 119–143.
- Bohn, T. J., Lettenmaier, D. P., Sathulur, K., Bowling, L. C., Podest, E., McDonald, K. C. & Friborg, T. 2007 Methane emissions from western Siberian wetlands: heterogeneity and sensitivity to climate change. *Environ. Res. Lett.* **2** (4), 045015.
- Brasington, J. & Richards, K. 1998 Interactions between model predictions, parameters and DTM scales for TOPMODEL. *Comput. & Geosci.* **24** (4), 299–314.
- Chang, C. H. & Lee, K. T. 2008 Analysis of geomorphologic and hydrological characteristics in watershed saturated areas using topographic-index threshold and geomorphology-based runoff model. *Hydrol. Process.* **22** (6), 802–812.
- Chen, J. & Kumar, P. 2001 Topographic influence on the seasonal and inter-annual variation of water and energy balance of basins in North America. *J. Climate* **14**, 1989–2014.
- Chen, X., Cheng, Q. B., Chen, Y. D., Smettem, K. & Xu, C. Y. 2010 Simulating the integrated effects of topography and soil properties on runoff generation in hilly forested catchments, South China. *Hydrol. Process.* **24** (6), 714–725.
- Clark, D. B. & Gedney, N. 2008 Representing the effects of subgrid variability of soil moisture on runoff generation in a land surface model. *J. Geophys. Res.* **113** (D10), D10111.
- Famiglietti, J. S. & Wood, E. F. 1994 Multiscale modeling of spatially variable water and energy balance processes. *Water Resour. Res.* **30** (11), 3061–3078.
- Freeman, T. G. 1991 Calculating catchment area with divergent flow based on a regular grid. *Comput. & Geosci.* **17**, 413–422.
- Giuseppe, M. & Aurelia, S. 1997 Information content theory for the estimation of the topographic index distribution used in TOPMODEL. *Hydrol. Process.* **11**, 1099–1114.

- Harris, A. & Hossain, F. 2008 Investigating the optimal configuration of conceptual hydrologic models for satellite-rainfall-based flood prediction. *IEEE Geosci. Remote S.* **5** (3), 532–536.
- Holmgren, P. 1994 Multiple flow direction algorithms for runoff modeling in grid-based elevation models: an empirical evaluation. *Hydrol. Process.* **8**, 327–334.
- Jenson, S. K. & Domingue, J. O. 1988 Extracting topographic structure from digital elevation data for geographic information system analysis. *Photogramm. Engin. Remote Sens.* **54**, 1953–1600.
- Koster, R. D., Suarez, M. J., Ducharne, A., Stieglitz, M. & Kumar, P. 2000 A catchment-based approach to modeling land surface processes in a general circulation model: 1. Model structure. *J. Geophys. Res.* **105** (D20), 24809–24822.
- Niu, G. Y. & Yang, Z. L. 2003 The versatile integrator of surface and atmosphere processes Part 2: evaluation of three topography-based runoff schemes. *Global Planet. Change* **38**, 191–208.
- Niu, G. Y., Yang, Z. L., Dickinson, R. E. & Gulden, L. E. 2005 A simple TOPMODEL-based runoff parameterization (SIMTOP) for use in global climate models. *J. Geophys. Res.* **110**, D21106.
- Pan, F., Peters-Lindard, C. D., Sale, M. J. & King, A. W. 2004 A comparison of geographical information systems-based algorithms for computing the TOPMODEL topographic index. *Water Resour. Res.* **40**, W06303.
- Pradhan, N. R., Ogden, F. L., Tachikawa, Y. & Takara, K. 2008 Scaling of slope, upslope area, and soil water deficit: implications for transferability and regionalization in topographic index modeling. *Water Resour. Res.* **44** (12), W12421.
- Qin, C., Zhu, A.-X., Pei, T., Li, B., Zhou, C. & Yang, L. 2007 An adaptive approach to selecting a flow-partition exponent for a multiple-flow-direction algorithm. *Int. J. Geogr. Inf. Sci.* **21**, 443–458.
- Quinn, P., Beven, K. J. & Lamb, R. 1995 The $\ln(\alpha/\tan \beta)$ index: how to calculate it and how to use it in the TOPMODEL framework. *Hydrol. Process.* **9**, 161–185.
- Quinn, P., Beven, K. J. & Planchon, O. 1991 The prediction of hillslope flow paths for distributed hydrological modeling using digital terrain models. *Hydrol. Process.* **5**, 59–79.
- Stieglitz, M., Rind, D., Famiglietti, J. & Rosenzweig, C. 1997 An efficient approach to modeling the topographic control of surface hydrology for regional and global modeling. *J. Climate* **10**, 118–137.
- Wilson, J. P. & Gallant, J. C. 2000 Primary topographic attributes. In: *Terrain Analysis: Principles and Applications* (J. P. Wilson & J. C. Gallant, eds.). Wiley, New York, pp. 51–85.
- Wolock, D. M. 1995 Effects of subbasin size on topographic characteristics and simulated flow paths in Sleepers River watershed, Vermont. *Water Resour. Res.* **31** (8), 1989–1997.
- Wolock, D. M. & McCabe, G. J. 1995 Comparison of single and multiple flow direction algorithms for computing topographic parameters in TOPMODEL. *Water Resour. Res.* **31** (5), 1315–1324.
- Yong, B., Ren, L. L., Chen, X., Zhang, Y., Zhang, W. C., Fu, C. B. & Niu, G. Y. 2009 Development of a large-scale hydrological model TOPX and its coupling with regional integrated environment modeling system RIEMS. *Chinese J. Geophys.* **52** (8), 1954–1965.
- Yong, B., Ren, L. L., Hong, Y., Wang, J. H., Gourley, J. J., Jiang, S. H., Chen, X. & Wang, W. 2010 Hydrologic evaluation of Multisatellite Precipitation Analysis standard precipitation products in basins beyond its inclined latitude band: a case study in Laohahe basin, China. *Water Resour. Res.* **46**, W07542.
- Zhou, Q. & Liu, X. 2002 Error assessment of grid-based flow routing algorithms used in hydrological models. *Int. J. Geogr. Inf. Sci.* **16**, 819–842.
- Zhou, Q. & Liu, X. 2004 Analysis of errors of derived slope and aspect related to DEM data properties. *Comput. & Geosci.* **30**, 369–378.
- Zushi, K. 2007 Regional estimation of Japanese cedar (*Cryptomeria japonica* D. Don) productivity by use of digital terrain analysis. *J. Forest Res.* **12** (4), 289–297.

First received 3 October 2009; accepted in revised form 26 August 2010. Available online December 2011